Structure-based engineering of Tor complexes uncovers different roles of two types of yeast TORC1s

Yoshiaki Kamada[1,2*], *Chiharu Umeda*[3], *Yukio Mukai*[3], *Hokuto Ohtsuka*[4], *Yoko Otsubo*[1], *Akira Yamashita*[1], *Takahiro Kosugi*[5,6,7,8*]

[1]Interdisciplinary Research Unit, National Institute for Basic Biology (NIBB), National Institutes of Natural Sciences (NINS), Okazaki, Aichi, 444-8585, Japan

[2] Basic Biology Program, SOKENDAI (The Graduate University for Advanced Studies), Hayama, Kanagawa, 240-0193, Japan

[3]Department of Frontier Bioscience, Nagahama Institute of Bio-Science and Technology, Nagahama, Shiga, 526-0829, Japan

[4]Laboratory of Molecular Microbiology, Graduate School of Pharmaceutical Sciences, Nagoya University, Nagoya, Aichi, 464-8601, Japan

[5]Research Center of Integrative Molecular Systems, Institute for Molecular Science (IMS), National Institutes of Natural Sciences (NINS), Okazaki, Aichi, 444-8585, Japan

[6]Exploratory Research Center on Life and Living Systems (ExCELLS), National Institutes of Natural Sciences (NINS), Okazaki, Aichi, 444-8585, Japan

[7]Molecular Science Program, SOKENDAI (The Graduate University for Advanced Studies), Hayama, Kanagawa, 240-0193, Japan

[8]PRESTO, Japan Science and Technology Agency, Kawaguchi, Saitama 332-0012, Japan

*To whom correspondence should be addressed. E-mail: yoshikam@nibb.ac.jp or takahirokosugi@ims.ac.jp

KEYWORDS: target of rapamycin, protein engineering, protein complex, lifespan, yeast

Abstract

Certain proteins assemble into diverse complex states, each having a distinctive and unique function in the cell. The target of rapamycin complex 1 (TORC1) plays a central role in signaling pathways for cells to respond to their environment, such as nutritional status. TORC1 is widely recognised for its association with various diseases. The budding yeast *Saccharomyces cerevisiae* has two types of TORC1s comprising different constituent proteins, Tor1- and Tor2-containing TORC1s but are considered to have the same function. Here, we rationally redesigned the complex states by structure-based engineering and constructed a Tor2 mutant to form TORC2 but not TORC1. Functional analysis of the mutant revealed that the two types of TORC1s induced different phenotypes-rapamycin, caffeine and pH dependences of cell growth and replicative and chronological lifespans. These findings are expected to provide further insights into various fields such as molecular evolution and lifespan.

Introduction

Various proteins assemble into complex states within cells, and a substantial proportion alters combinations of constituent proteins to proficiently exert their functions in the appropriate spatiotemporal context. Target of rapamycin (Tor), an evolutionarily conserved protein kinase, plays a pivotal role in eukaryotic cell signalling pathways. It responds to changes in the extracellular environment, such as changes in nutritional status, and is associated with various diseases and lifespans (Liu & Sabatini, 2020; Loewith & Hall, 2011). Tor forms two distinct complex dimers, Tor complex 1 and 2 (TORC1 and TORC2) (Loewith *et al*, 2002). They comprise different several constituent proteins, resulting in exerting different functions (Fig. 1A) (Liu & Sabatini, 2020; Loewith & Hall, 2011). In *S. cerevisiae*, a serine/threonine protein kinase, Tor1, assembles into TORC1 with the main partner Kog1 (yeast counterpart of Raptor) and other partner proteins such as Lst8. Another kinase protein, Tor2, assembles into not only TORC1 but also TORC2 with the main partner Avo3 (yeast counterpart of Rictor) and other proteins, e. g. Lst8, Avo1 and Avo2 (Loewith *et al.*, 2002). Namely, there are two types of *S. cerevisiae* TORC1s which are composed of Tor1 or Tor2 (hereafter referred to as Tor1-TORC1 and Tor2-TORC1), whereas other species, such as mammals and the fission yeast, *Schizosaccharomyces pombe*, have only one type of TORC1 (Fig. 1A) (Otsubo *et al*, 2017).

To the best of our knowledge, functional differences between Tor1-TORC1 and Tor2-TORC1 have not yet been studied. Tor2-TORC1 has been ignored because the amount of Tor2-TORC1 in cells is lower than that of Tor1-TORC1 (Loewith *et al.*, 2002; Reinke *et al*, 2004). Moreover, the functions are thought to be the same because Tor1 is a homologue of Tor2 with high sequence identity (66.2%) and the same ligands are phosphorylated by both Tor1-TORC1 and Tor2-TORC1 (Kunz *et al*, 1993). However, these complexes exhibit several interesting assembly properties.

Tor2 assembles into both complex states, whereas Tor1 does not assemble into TORC2. There is also no chimeric TORC1 dimer which contains both Tor1 and Tor2; in a TORC1 dimer, only either Tor1 or Tor2 is included (Loewith *et al.*, 2002; Reinke *et al.*, 2004; Takahara *et al*, 2006).

TORC1 and TORC2 activity in *S. cerevisiae* is essential for cell growth (Loewith & Hall, 2011). *TOR1* deletion is not lethal because only Tor1-TORC1 is deleted and Tor2-TORC1 remains. The *tor1*Δ strain has been under intense investigation. It has been shown that the cell lifespan of *tor1*Δ cells is extended (Kaeberlein *et al*, 2005), because partial inhibition of TORC1 mimics calorie restriction, an important factor of longevity (Lin *et al*, 2000). Inhibition of TORC1 using drugs, such as rapamycin or Torin-1, also leads to longevity in various organisms, including yeast, nematodes, flies, and rodents. (Dabrowska *et al*, 2022; Folch *et al*, 2018; Harrison *et al*, 2009; Martinez-Miguel *et al*, 2021; Ohtsuka *et al*, 2021b; Rodríguez-López *et al*, 2020). For lifespan, Tor1-TORC1 is expected to have a function similar to that of TORC1s in other species. However, the function of Tor2-TORC1 function is unclear. *TOR2* deletion is lethal because only Tor2 assembles into TORC2 (Kunz *et al.*, 1993; Loewith *et al.*, 2002); this could be one of the reasons why Tor2-TORC1 has never been studied.

Studies on Tor complexes by domain exchange did not show the differences between Tor1-TORC1 and Tor2-TORC1; they performed the experiments to identify important interactions for assembling complex states (Hill *et al*, 2018; Tsverov *et al*, 2022). If high-resolution three-dimensional structures are solved using X-ray or cryo-EM, important interactions can be uncovered. Moreover, a comparison of the three-dimensional structures of *S. cerevisiae* Tor1-TORC1 and Tor2-TORC1 may provide clues about their functions. However, high-resolution structures have not yet been obtained.

Recently, remarkable development of computational protein structure prediction and protein

design methods has been achieved (Baek *et al*, 2021; Dauparas *et al*, 2022; Huang *et al*, 2016; Jumper *et al*, 2021). Using computational methods, native proteins have been redesigned and their functions have been successfully controlled. For example, artificial activation or inactivation of G protein-coupled receptors and cyclic GMP-AMP synthase by state-targeting stabilisation have been reported (Chen *et al*, 2020; Dowling *et al*, 2023). We have also previously controlled the concerted function, rotation, of a rotary molecular motor, V_1-ATPase, using a novel approach based on computational protein design methods (Kosugi *et al*, 2023). Here, based on predicted structural models for protein complexes whose experimental structures are unavailable, we engineered a constituent protein to change the pattern of possible combinations and attempted to uncover the biological functions of a protein complex in cells.

In this study, we designed a Tor2 mutant protein which could not form TORC1 but could form TORC2 (Fig. 1B) by structure-based engineering. Mutant strains of *TOR2* showed differences for several phenotypes with those of the *tor1*Δ strain-rapamycin, caffeine and pH dependences of cell growth and replicative and chronological lifespans. These results revealed that the several characteristics of Tor2-TORC1 were different from those of Tor1-TORC1. Based on the differences in their roles, we propose new perspectives for research on the molecular evolution and lifespan.

Results

Structure-based engineering of Tor2 to lose its ability to assemble to TORC1, but retain its ability to maintain the TORC2 assembly

To engineer Tor2 not to assemble to TORC1 but to maintain the TORC2 assembly based on the structures, we focused on the interactions between Tor2 and the unique components of each complex–Kog1 for Tor2-TORC1 and Avo3 for TORC2. We aimed to eliminate the interaction of Tor2 with Kog1 and retain it with Avo3 by structure-based engineering. Therefore, reasonable structures for Tor2-TORC1 and (Tor2-)TORC2 are required. However, high-resolution structures of Tor2-TORC1 and TORC2 from *S. cerevisiae* have not been reported, except for a recently resolved cryo-EM structure of the TORC1 inactive condensate, TOROID (Prouteau *et al*, 2023). Both cryo-EM structures of mTORC1 and mTORC2 have been reported at approximately 3.2 Å resolution (Scaiola *et al*, 2020; Yang *et al*, 2017). Therefore, by superimposing homology models of each constituent protein (Tor2, Kog1, and Avo3) from *S. cerevisiae* on the human Tor complex structures, we computationally modelled a dimer of the Tor2 and Kog1 protein complex as Tor2-TORC1, and a dimer of the Tor2 and Avo3 protein complex as TORC2 (Fig. 2). By comparing these two model complex structures, we found a design target region in Tor2 that interacted with Kog1 but not with Avo3; note that other constituent proteins, LST8 and Avo2, also do not interact with this region. This region contacts loop structures of Kog1 which are not in orthologues from other species, *S. pombe* or humans (the sequence alignments are shown in Appendix Fig. S1); this loop structures are expected to contribute to TORC1 assembly of *S. cerevisiae* Tor2. In the design target region of Tor2, nine amino acid residues (A740, A742, K768, A772, A775, A777, L781, F817, and K818) within the HEAT domain were selected and mutated to crash with the characteristic loop region of Kog1 and to stabilize the surface exposed to solvent; hydrophobic

and charged residues were mutated to a larger and hydrophilic residue, glutamine, and to larger amino acids with the same charge, respectively. As shown in Fig. 3A, seven combinations of the mutations—K1, K2, K3, K12, K13, K23 and K123—were experimentally validated.

Engineered Tor2 mutant maintains TORC2 activity but does not have TORC1 activity

Tor2-TORC1 and TORC2 activities in the seven mutant strains were verified using a cell-based assay. The TOR2 mutant plasmids cloned into pRS314 (TRP1) vector were transformed into *TOR1 tor2*Δ and *tor1*Δ *tor2*Δ strains, harbouring the pRS316(URA3)[TOR2] plasmid. The transformants were streaked onto YEPD (control) or 5-FOA plates to select a *ura*$^-$ cell which loses the URA3-maker wild-type TOR2 plasmid and harbuored only the mutated TOR2 plasmid. Growth on 5-FOA plates was used to evaluate the function of TORC2 (*TOR1 tor2*Δ strain) and TORC1 TORC2 (*tor1*Δ *tor2*Δ strain) (Fig. 3B) because the loss of either TORC1 or TORC2 activity is lethal for cells. For example, K1, K2, K3, K13, and K23 transformants grew on 5-FOA plates in both *TOR1 tor2*Δ and *tor1*Δ *tor2*Δ background as well as the wild type (Fig. 3A and B). In contrast, the K12 and K123 transformants grew on 5-FOA only in *TOR1 tor2*Δ background, indicating that these two *TOR2* mutants do not function as TORC1. These results suggest that the two strains, K12 and K123, exhibit activities as expected from the design.

To further characterise the Tor2(K12) and (K123) mutants, their TORC1 and TORC2 complex-forming abilities were evaluated by co-immunoprecipitation (Fig, 4A-C). Analysis of Tor2-TORC1, in which the HA-tagged Tor2(K12) mutant was pulled down together with FLAG-tagged Kog1, indicated that the Tor2(K12) mutant largely loses its ability to form a Tor2-TORC1 complex with Kog1. However, analysis of TORC2 by FLAG-tagged Avo3 together with cell-based assays indicated that the K12 mutant maintained sufficient Tor2-TORC2 forming ability to

function as TORC2. When the same amount of TORC2 was immunoprecipitated for the *in vitro* TORC2 kinase assay, Tor2-TORC2 kinase activity was found to be similar between the wild-type and Tor2(K12) mutant, confirming that mutation sites in K12 did not affect the specific activity of TORC2 (a similar result was obtained by another method using ATPγS as a substrate, as shown in Appendix Fig. S2). These results show that the Tor2(K12) mutant was successfully designed as we expected; in Tor2(K12) mutant cell, Tor2-TORC1 formation is largely compromised while (Tor2-)TORC2 formation is well conserved. HA-tagged Tor2(K123) protein was barely detected in the cell lysate, while it was detected in denatured conditions (Appendix Fig. S3); therefore, we could not perform co-immunoprecipitation analysis. This complex is probably more fragile than the Tor2(K12) mutant complex, although it form the TORC2 and has TORC2 activity in cells. Therefore, for further experiments, we focused on the Tor2(K12) mutant and investigated functions of the two types of TORC1s by comparing the K12 strain (Tor2-TORC1 was almost lost in the cell) with the *tor1*Δ strain (Tor1-TORC1 was lost).

Phenotypes of *tor1*Δ and *tor2* mutant strains are different from each other

First, the *in vivo* TORC1 kinase activities in *tor1*Δ and *tor2*(K12) strains were estimated by the phosphorylation states of TORC1 substrates, Atg13 or Sch9 (Kamada *et al*, 2010; Urban *et al*, 2007). In both mutant strains, the activity of TORC1 was similar to that of wild-type strain (Fig. 4D). Therefore, even if either of TORC1s is lost, the TORC1 kinase activity of the major ligands is maintained. Incidentally, the TORC2 activity, kinase activity for Mpk1 (Fig. 4E) in cells, and actin organisation in cells (Kamada *et al*, 2005) (Fig. 4F) were also completely maintained. Therefore, Tor2(K12)-TORC2 did not affect the phenotypes observed at 30 °C. The *tor2*(K12) strain showed growth defects at 37°C (Appendix Fig. S4).

Next, we examined the cell phenotypes of the *tor2*(K12) and *tor1*Δ strains in the presence of

TORC1 inhibitors (Fig. 5A). As previously reported, the *tor1*Δ strain is more sensitive than the wild-type strain to rapamycin, a selective inhibitor of TORC1, and caffeine, an inhibitor of TORC1 (Reinke *et al*, 2006; Sekiguchi *et al*, 2014), than those of the wildtype. Interestingly, the *tor2*(K12) strain had a different phenotype from the *tor1*Δ strain and was even more sensitive to rapamycin and caffeine than the *tor1*Δ strain. The sensitivity of the *tor1*Δ strain can be explained by a decrease in the total amount of TORC1. However, the hypersensitivity of the *tor2*(K12) strain cannot be explained by a decrease in TORC1, because the amount of Tor2-TORC1 is generally lower than that of Tor1-TORC1 (Loewith *et al.*, 2002; Reinke *et al.*, 2004). This result indicated that Tor2-TORC1 is distinct from Tor1-TORC1 in terms of its response to TORC1 inhibitors. Moreover, under several pH conditions, growth of the *tor2*(K12) and *tor1*Δ strains was observed (Fig. 5B). The *tor1*Δ cell grew better than the wildtype at even high pH (pH 8.0~8.5). In contrast, *tor2*(K12) cells grew poorly at a high pH (pH 8.0) and did not grow at higher pH (pH 8.5). This result also indicates that Tor1-TORC1 has different role from Tor2-TORC1.

Finally, replicative and chronological lifespans were measured for the wild-type, *tor1*Δ and *tor2*(K12) strains (Fig. 5C and D). The *tor1*Δ strain had a longer replicative lifespan than that of the wild-type strain, as previously reported (Kaeberlein *et al.*, 2005). The replicative lifespan of the *tor2*(K12) strain was similar to that of the wildtype, although it seemed slightly shorter. The mean life spans of the wild-type, *tor1*Δ and *tor2*(K12) strains are 23.0, 28.3, and 20.7, respectively. All strains had chronological lifespans similar to their replicative lifespans: chronological lifespan of the *tor2*(K12) strain was similar to that of the wild-type strain, while the *tor1*Δ strain had longer chronological lifespans than the wild-type strain. Both lifespan results suggest that the roles of Tor1-TORC1 and Tor2-TORC1 are different from each other. It is possible that the *tor2*(K12) strain is less affected because of the lower amount of Tor2-TORC1. However, since the TORC1

194 activity itself is almost the same in both the same in both the *tor2*(K12) and *tor1Δ* strains (Fig. 4D),
195 it is more likely that Tor1-TORC1 and Tor2-TORC1 contribute in different ways to lifespan
196 regulation.

197 These phenotypic observations indicate that two types of TORC1s, namely Tor1-TORC1 and
198 Tor2-TORC1, not only have common and essential functions, but also have distinct functions.

Discussion

We engineered *S. cerevisiae* Tor2 based on computationally modelled Tor2-TORC1 and TORC2 structures. Through various cell biology and biochemical experiments, it was verified that the Tor2(K12) mutant maintains TORC2 activity but does not have TORC1 activity, as designed. Because only TORC1 activity is deleted from Tor2, the *tor2* mutant provides a strain without Tor2-TORC1 function, which is not created by the deletion of a gene because both TORC1 and TORC2 are essential for cells. By comparing the phenotypes of the *tor2* mutant strain with the *tor1*Δ strain, we found Tor2-TORC1 has distinct functions from that of Tor1-TORC1. Further research, for example, by solving and comparing high-resolution structures, could uncover the differences between Tor1-TORC1 and Tor2-TORC1 in detail.

In this study, we successfully altered the combinations of constituent proteins in a protein complexes using structure-based engineering, which has contributed to uncovering the biological function of the protein complexes. Various proteins form complex states in cells, many of which alter the combination of constituent proteins and exert their functions at the correct place and time. Our approach, which artificially engineered a combination of constituent proteins, enabled us to control celllar phenotypes and uncover the roles of protein complexes. However, a reasonable structural model is essential for the structure-based engineering. In this study, we designed mutants based on model complex structures predicted computationally by homology modeling and not on the experimental structures. Even if an experimental structure of the homologue protein is not available, AlphaFold 2 (Jumper *et al.*, 2021), a high-accuracy protein structure prediction program using deep learning, has been developed, and we can use high-quality structural data for any proteins that we are interested in designing; note that experimental structures are better for designing mutants when they have been solved at the high resolution. Therefore, our approach

applies to any target protein, and we could engineer native proteins based on their structure and uncover their biological functions.

The phenotypic difference between the K12 and *tor1*Δ strains not only indicates that the role of Tor1-TORC1 is not the same with that of Tor2-TORC1 but also provides more detailed information about the characteristics of Tor1-TORC1 and Tor2-TORC1. The higher sensitivity of the *tor2*(K12) mutant strain to TORC1 inhibitors may indicate that Tor2-TORC1 has a lower binding affinity or a more robust response to the inhibitors than Tor1-TORC1. The pH dependence of cell growth might be related to the activation of vacuolar-type ATPase (V-ATPase), an ATP-driven proton pump, by TORC1. Transport across the plasma membrane by V-ATPase controls the cytoplasmic pH condition and deletion of V-ATPase causes to deceleration of growth at high pH conditions (Kane, 2006; Nelson & Nelson, 1990), suggesting that high V-ATPase activity might enable growth at high pH conditions. The activity of mammalian V-ATPase is dependent on the activation of mTORC1; the inactivation of mTORC1 regulates the formation of a complete and active complex state (Ratto *et al*, 2022). Therefore, it is expected that *S. cerevisiae* TORC1 activity also affects the activation of V-ATPase, and its inactivation induces cell growth under alkali pH conditions. Our results were consistent with this expectation; the *tor1*Δ strain (permanent inactivation of Tor1-TORC1) grew under high pH conditions. In contrast, the K12 strain (almost permanently inactivated Tor2-TORC1) exhibited the opposite phenotype. Although these results should be investigated in more detail; future research on these two strains may contribute to our understanding of the mechanism of V-ATPase activation by TORC1.

The findings obtained from this study could provide clues to research the evolution of Tor2. The longer lifespan of the *tor1*Δ strain is the same phenotype with inhibition of mTORC1 or *S. pombe* TORC1, as previously reported (Harrison *et al.*, 2009; Rodríguez-López *et al.*, 2020). The

pH dependence of growth of the *tor1*Δ strain (no Tor1-TORC1) is expected to be induced by the function, probably corresponding to mTORC1. Therefore, *S. cerevisiae* Tor1-TORC1 corresponds to TORC1s from other species, as mentioned in the Introduction. However, our results indicate that the role of Tor2-TORC1 is not the same with those of Tor1-TORC1 in *S. cerevisiae* and TORC1s in other species; it is a characteristic TORC1 of *S. cerevisiae*. This result also provides us information on the evolution of Tor. A simple hypothesis is *S. cerevisiae* Tor1-TORC1 is a special and later emergent one in the process of evolution because *S. cerevisiae* Tor2 forms both TORC1 and TORC2, similar to mTOR. However, our results indicate that Tor2-TORC1 is unique and a simple hypothesis of the evolution process is not reasonable. By further investigation of Tor2-TORC1, we could approach the evolution of Tor2.

We also obtained important findings regarding lifespan researches. Lifespan experiments showed that the *tor2*(K12) strain (almost no Tor2-TORC1) had a lifespan similar to that of the wildtype, although the *tor1*Δ strain (no Tor1-TORC1) had a longer lifespan. This result suggests that Tor1-TORC1 and Tor2-TORC1 had shortened and unaffected lifespans, respectively. By further investigating the differences between Tor1-TORC1 and Tor2-TORC1, we can uncover *S. cerevisiae* Tor2-TORC1's function in more detail. This knowledge might enable us to create a mTORC1 similar to *S. cerevisiae* Tor2-TORC1 and to extend the lifespan by replacing the mTORC1 with a novel one in mammals without inhibiting the activity of mTORC1. This will enable the control of the lifespans of mammals.

Materials and Methods

Design protocol for Tor2 mutant

The model structures of Tor2-TORC1 and TORC2 were created using following procedure. Homology models of Tor2, Kog1, and Avo3 were individually generated using the SWISS-MODEL server (Waterhouse *et al*, 2018). The model structures were superimposed on the mTORC1 (PDB ID: 6BCX) and mTORC2 (PDB ID: 6ZWM) cryo-EM structures. To remove crashes between the atoms of each component, the components were shifted slightly from each other and, the side chains were repacked using the Rosetta protein design software (Leaver-Fay *et al*, 2011). These two model complex structures were compared and candidate residues for mutations that contribute to binding to Kog1 in Tor2-TORC1 and not to Avo3 in TORC2 were selected. The hydrophobic residues of the candidates were mutated to a larger hydrophilic but uncharged amino acid, glutamine. Positively or negatively charged residues were mutated to larger amino acids with the same charge, for examples, Lys to Arg. Several combinations of the candidate residues were experimentally validated.

Strains, plasmids, media and genetic methods

The yeast strains, plasmids and DNA primers used in this study are listed in Appendix Tables S1, S2, and S3. Standard techniques have been used to manipulate yeast (Kaiser, 1994; Longtine *et al*, 1998). Antibodies against HA-epitope (16B12, COVANCE, x5,000 dilution), Flag-epitope (M2, Sigma, x5,000 dilution), phospho-p44/42 (#9101, Cell Signaling, x3,000 dilution), and thiophosphate ester-specific RabMb (Abcam, x5,000 dilution) were used as primary antibodies for immunoblotting at the indicated concentrations. Antibodies against Atg13 (x3,000 dilution) were

used as described previously (Kamada *et al*, 2000). The FLAG-tagged AVO3 strain was generated following a previously described protocol (Longtine *et al.*, 1998; Sung *et al*, 2005)

Creating, cloning, and cell-based assay for *TOR2* mutants

TOR2 mutants were generated and cloned using the designated gap repair cloning (GRC) method (Chino *et al*, 2010; Ma *et al*, 1987). The overall procedure is presented in Appendix Fig. S5. First, site-directed mutated TOR2 fragments were amplified by PCR using specific DNA primers (Appendix Fig. S5A, Appendix Table. S3). Next, these (2 or 3) DNA fragments were mixed and transformed into yeast cells with a linearised pRS314 vector (Appendix Fig. S5B). The plasmids created by GRC were rescued from yeast transformants.

The resultant TOR2 mutant plasmids were transformed into *TOR1 tor2*Δ (YYK1411) and *tor1*Δ *tor2*Δ (YYK1412) strains, harbouring pRS316[TOR2] plasmid. The transformants were streaked onto 5-FOA plates to select a *ura3* cells which loses the URA3-maker wild-type TOR2 plasmid and harboured only the mutated TOR2 plasmid. Growth on 5-FOA plates was used to evaluate the functions of TORC2 (*TOR1 tor2*Δ strain) and TORC1 TORC2 (*tor1*Δ *tor2*Δ strain). A YEPD plate was used as a growth control.

As for the integration of *tor2*(K12) allele into the *TOR2* locus, the pRS314[TOR2(K12)] plasmid created above was cloned into BYP9689 (pBSBleMX), and HindIII-HindIII (1.9kb, encoding FAT-FRB-kinase domain) region of the insert was deleted to make pBSBleMX[TOR2(K12) H3Δ]. The resulting plasmid was linearised by BamHI digestion and transformed into the BY4741 strain to generate the *tor2*::BleMX::*tor2*(K12) mutant. The phenotype of this strain was examined as shown in Appendix Fig. S6. This strain (YYK1551) was used for lifespan assay.

Immunoprecipitation of TORC1 and TORC2

Immunoprecipitation of the Tor complexes was performed as previously described (Kamada, 2017). For the TORC1 experiment, YYK1467 and YYK1530 (^{HA}TOR2 ^{Flag}KOG1 strains) and for TORC2 experiment, YYK1464 and YYK1528 (^{HA}TOR2 AVO3^{Flag} strains) were used. Yeast cells grown in YEPD at 30 °C overnight were collected and resuspended in Z-buffer (50 mM Tris-HCl pH7.5, 1 M sorbitol) containing 0.01 mg/OD_{600} cells zymolyase 100T (Nacalai Tesque). These were converted to spheroplasts with 30 min incubation at 30 °C. The spheroplasts were harvested, washed by Z-buffer once, and suspended in 10 µl/OD_{600} cells ice-cold IP-buffer (1xPBS, 2 mM $MgCl_2$, 1 mM Na_3VO_4, 7.5 mM *p*-nitrophenyphosphate (*p*NPP), 10 mM β-mercaptoethanol, 1% Tween-20), containing protease inhibitors (40 µg/ml leupeptin, 80 µg/ml aprotinin, 20 µg/ml pepstatinA, 200 µg/ml 4-(2-Aminoethyl) benzenesulfonyl fluoride hydrochloride (AEBSF), and 1 mM PMSF). The cell suspension was gently mixed and incubated on ice for 5 min to break spheroplasts. The lysate was centrifuged 15,000*xg* at 4 °C for 10 min twice, and the clear lysate (700 µl) was incubated with 15 µl of Dynabeads protein G (Invitrogen) bound with or without (control) 1 µl of anti-Flag antibody (M2, Sigma) 4 °C for 2 h with gentle rotation. The beads were transferred into fresh microfuge tubes and washed thrice with 1xPBS or Tes-buffer.

In vitro TORC2 kinase assay

TORC2 kinase activity was evaluated using RI and non-RI kinase assays as described previously (Allen *et al*, 2007; Kamada, 2017; Kamada *et al.*, 2005). The resultant immunocomplex was washed once, suspended in 24 µl of Tes-buffer (25 mM Tes-KOH pH7.25, 100 mM KCl, 10 mM $MgCl_2$) containing 2 µg of the substrate (^{His6}4EBP1), and preincubated at 30 °C for 5 min. In the RI kinase assay, the reaction was initiated by the addition of 3 µl of 2 mM [γ-^{32}P]ATP (222

TBq/mmol Perkin Elmer) to the mixture (final concentration, 0.2 mM, 0.2 MBq/reaction), and the reaction mixture (final volume 30µl) was further incubated at 30 °C for 10 min. The reaction was terminated by adding of 15 µl of 4x SDS-PAGE sample buffer and incubating at 65 °C for 5 min. The samples (20 µl) were subjected to SDS-PAGE (12.5%), and the phosphorylated proteins were analysed using autoradiography and a BAS5000 (Fuji Film). In the non-RI assay, the reaction was initiated by adding 6 µl of 1 mM ATPγS (Abcam) to the mixture (final concentration, 0.2 mM), and the reaction mixture (final volume, 30µl) was further incubated at 30 °C for 20 min. The reaction was terminated by adding 3 µl of 250 mM EDTA. The protein in the reaction mixture was alkylated with 1.7 µl of 50 mM *p*-nitrobenzyl mesylate (*p*NBM, 2.7 mM, Abcam) at room temperature for 80 min. The sample was added to 12 µl of 4x SDS-PAGE sample buffer and incubated at 95°C for 2 min, and a 20 µl aliquot was subjected to SDS-PAGE (12.5%). The phosphorylated substrate was analysed by immunoblotting using thiophosphate ester-specific RabMb (Abcam) according to the manufacturer's protocol.

In vivo kinase analyses

Immunoblotting was performed as previously described (Kamada, 2017). Yeast cells harbouring YEp352[ATG13], YCplac33[^{HA}SCH9], or YEp352[MPK1^{HA}] grown in YEPD medium at 30 °C. For the nitrogen starvation treatment, cells were collected, washed thrice with distilled water, transferred to synthetic dextrose (SD) (-N) medium (0.17% yeast nitrogen base without ammonium sulfate and amino acids, 2% glucose), and incubated for 30 min. Cells (10 OD_{600} units) were collected and fixed with 100 µl of ice-cold alkaline solution (0.2 N NaOH and 0.5% β-mercaptoethanol). After 5 min of incubation on ice, 10 µl of 1.8 M NaOAc pH5.2 and 1 ml of ice-cold acetone were added to the sample and incubated at -20 °C to precipitate the proteins. The

355 protein samples were precipitated with a microfuge for 5 min, air-dried, suspended in 100 µl of
356 SDS-PAGE sample buffer, and incubated at 65 °C for 15 min. The samples were thoroughly
357 dissolved by sonication and subjected to sodium dodecyl sulfate-polyacrylamide gel
358 electrophoresis. For immunoblotting, peroxidase-conjugated goat anti-rabbit IgG (H+L) or sheep
359 anti-mouse IgG (H+L) (Jackson ImmunoResearch) was used as a secondary antibody (x10,000
360 dilution). Immobilon Forte Western HRP (Merck) and Light-Capture II (ATTO) were used for
361 signal detection.
362

363 ## Actin staining

364 Staining for actin was performed and observed as described previously (Kamada *et al.*, 2005;
365 Nakano *et al*, 2011). YEPD-grown cells were fixed for 30 min by the direct addition of 37%
366 formaldehyde stock to a final concentration of 5%. Fixed cells were collected, washed with 1xPBS
367 thrice, and then bodipy-phallacidin (Molecular Probes) was added for 2 h at room temperature to
368 stain F-actin as previously described (Kaiser, 1994). Fluorescence and bright-field images were
369 captured using a personal DV microscope (Applied Precisions). Fluorescence images were
370 acquired in 20 serial sections along the z-axis at intervals of 0.2 mm. All images were 3-
371 dimensionally deconvolved and stacked using the quick projection algorithm in the SoftWoRx
372 software (Applied Precisions).
373

374 ## Replicative life-span assay

375 The replicative lifespans was measured for the wild-type (BY4741), *tor1* Δ (YYK332), and
376 *tor2*(K12) (YYK1551) strains. Replicative lifespan was assayed as previously described
377 (Nakajima *et al*, 2020). Yeast cells were thawed from the frozen stock and streaked onto YEPD

agar plates. After 2 days, a single colony was spread onto a YEPD agar plate, and the cells were grown at 30 °C overnight. The next day, cells were transferred again to a fresh YEPD agar plates and grown overnight. Using a micromanipulator, 48 cells were arrayed on a plate and allowed to undergo one or two divisions. Virgin cells were then selected and subjected to lifespan analysis. Except during manipulation, the plates were sealed with Parafilm, incubated at 30 °C during the day and stored at 4 °C at night to avoid excessive budding. Daughter cells were removed by gentle agitation using a dissecting needle and scored every 2 h. For each of the 48 cell lines, buds from each mother cell were counted for at least 3 days until the division of living cells ceased. The mean replicative lifespan and the *p*-value were calculated using the Wilcoxon rank-sum test and weighted log-rank test relative to the wild-type strain, BY4741.

Chronological life-span assay

The same cell strains as those used in the replicative lifespan assay were used. To measure cell survival, cells were grown in SD liquid medium, sampled during each growth phase, and plated on yeast extract agar plates after dilution (Ohtsuka *et al*, 2021a). After 4–7 days at 30 °C, using colony-forming units, the number of viable cells in 1-mL aliquots of culture was determined and divided based on the cell turbidity at each sampling time. Cell growth was then monitored according to the turbidity determined using a Bactomonitor (BACT-550) equipped with a 600 nm filter (Nissho Electric).

To measure the chronological lifespan, the wild-type (BY4741), *tor1* Δ (YYK332), and *tor2*(K12) (YYK1551) strains were cultured in SD medium with 240 mg/L leucine, 80 mg/L uracil, 80 mg/L histidine, and 80 mg/L methionine ($n = 3$).

Acknowledgements

We thank Dr. T. Maeda for helpful suggestions, Dr. H. Moriya for his technical advice, Dr. J. Broach for his generous gift of the TOR2 plasmid, Y. Ito and S. Kawai for technical assistance, and the members of the Tokai Tor Conference (ToToCo) for general discussions. We thank the NIBB Center for Radioisotope Facilities and the NIBB Trans-Omics Facility for their technical support. We also thank the National BioResource Project Yeast for the plasmid distribution. This work was supported by the NINS program for cross-disciplinary study (Grant Number 01312108 to Y. K., Y. O., A. Y. and, T. K.) and by the grant of Joint Research by the National Institutes of Natural Sciences (NINS) (NINS program No, 01112205 to Y. K., Y. M., H. O., Y. O., A. Y. and, T. K.) and by the Japan Science and Technology Agency (JST) Precursory Research for Embryonic Science and Technology (PRESTO, Grant Number JPMJPR20E6 to T. K.) and by a Grant-in-Aid for Scientific Research (C) from the Ministry of Education, Culture, Sports, Science and Technology of Japan (to HO) (JP21K05363).

Author Contributions

T. K. conceived and conceptualized this project in discussion with Y. K., Y. O., and A. Y. Y. K. and T. K. designed the research in discussion with Y. O. and A. Y. T. K. performed to generate computational structure models and designed Tor2 mutations. Y. K. and T. K. prepared plasmid constructs. Y. K. performed cell-based screening, co-immunoprecipitation analyses, kinase assays and phenotype investigations for the TORC1 inhibitors. T. K. investigated phenotypes at several pH conditions. Y. K., Y. O., and A. Y. performed actin staining. C.U. and Y. M. performed replicative life-span assay. H. O. performed chronological life-span assay. Y. K. Y. O. A. Y., and

T. K. wrote the initial manuscript. All authors discussed the results and contributed to the final manuscript.

Competing Financial Interests

The authors declare no competing financial interests.

Data Availability

The yeast strains and plasmids used in this study are available from the authors upon request.

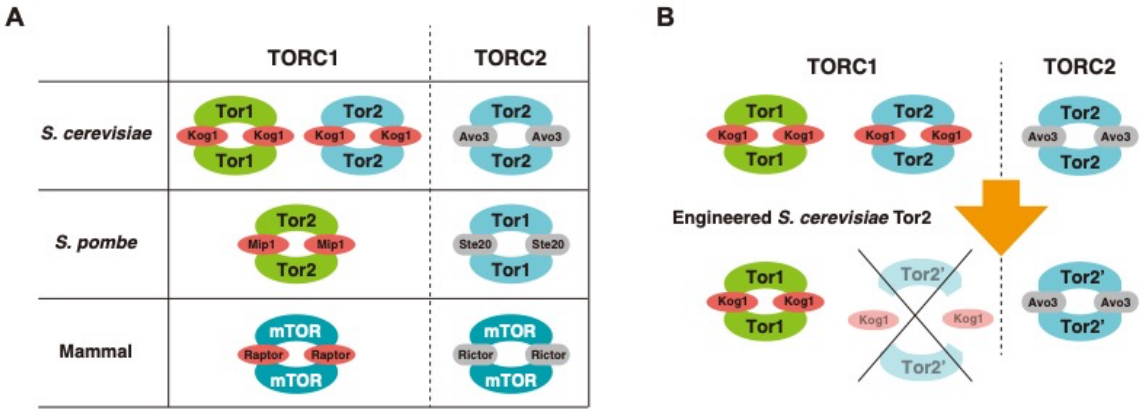

Fig. 1. Strategy to compare two types of TORC1 in *S. cerevisiae*.

A. Orthologue proteins which constitute TORC1s and TORC2s in several species. Only *S. cerevisiae* has two types of TORC1, namely Tor1- and Tor2-containing TORC1s (Tor1-TORC1 and Tor2-TORC1).

B. Tor2-TORC1 in *S. cerevisiae* is deleted by engineering Tor2 to maintain the binding ability with Avo3 and not with Kog1. In these figures, Lst8 is omitted.

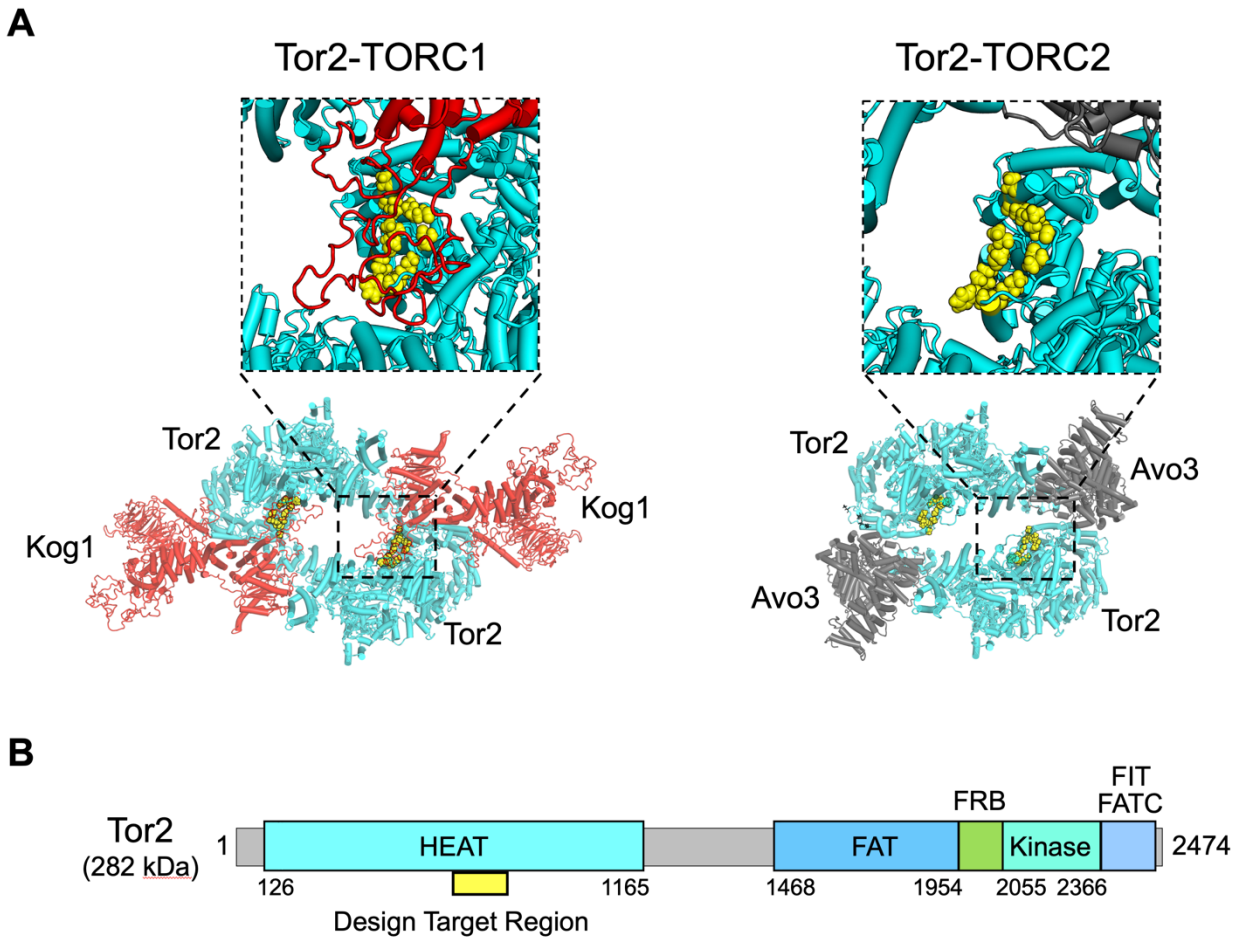

Fig. 2. Design target region in Tor2 found by comparing two model structures.

A. Model structure of Tor2-TORC1 (left) and Tor2-TORC2 (right) (Lst8 is omitted). The amino acid residues in the design target region, with which Kog1 interacts but Avo3 does not, are shown as yellow spheres.

B. Design target region (yellow) on the primary sequence of Tor2. The region is on the Tor2 HEAT domain.

A

126 *Designed TOR2* 1165

TOR2 HEAT domain

	A740	A742	K768	A772	A775	A777	L781	F817	K818	TORC1 activity	TORC2 activity
K1	Q	Q								✓	✓
K2			R	Q	Q	Q	Q			✓	✓
K3								Q	R	✓	✓
K12	Q	Q	R	Q	Q	Q	Q				✓
K13	Q	Q						Q	R	✓	✓
K23			R	Q	Q	Q	Q	Q	R	✓	✓
K123	Q	Q	R	Q	Q	Q	Q	Q	R		✓

B

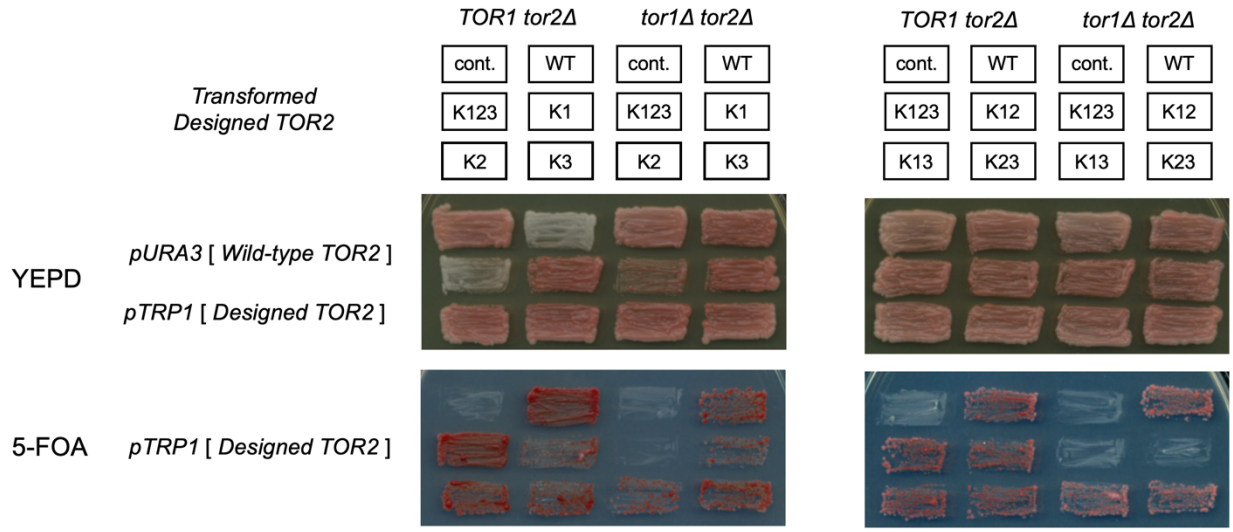

Fig. 3. Cell-based assay for the designed Tor complexes having no TORC1 function and retaining TORC2 function.

A. Mutation site and amino acid type of designed Tor2s. A summary of the cell-based assay is also shown.

B. Cell-based activity assay of Tor complexes with several designed *TOR2* mutants; K1, K2, K3, K12, K13, K23, and K123. Cells were patched onto YEPD (top) and 5-FOA (bottom) plates and incubated for 2 days at 30 ºC. K12 and K123 have no TORC1 activity and retain TORC2 activity, respectively, as designed.

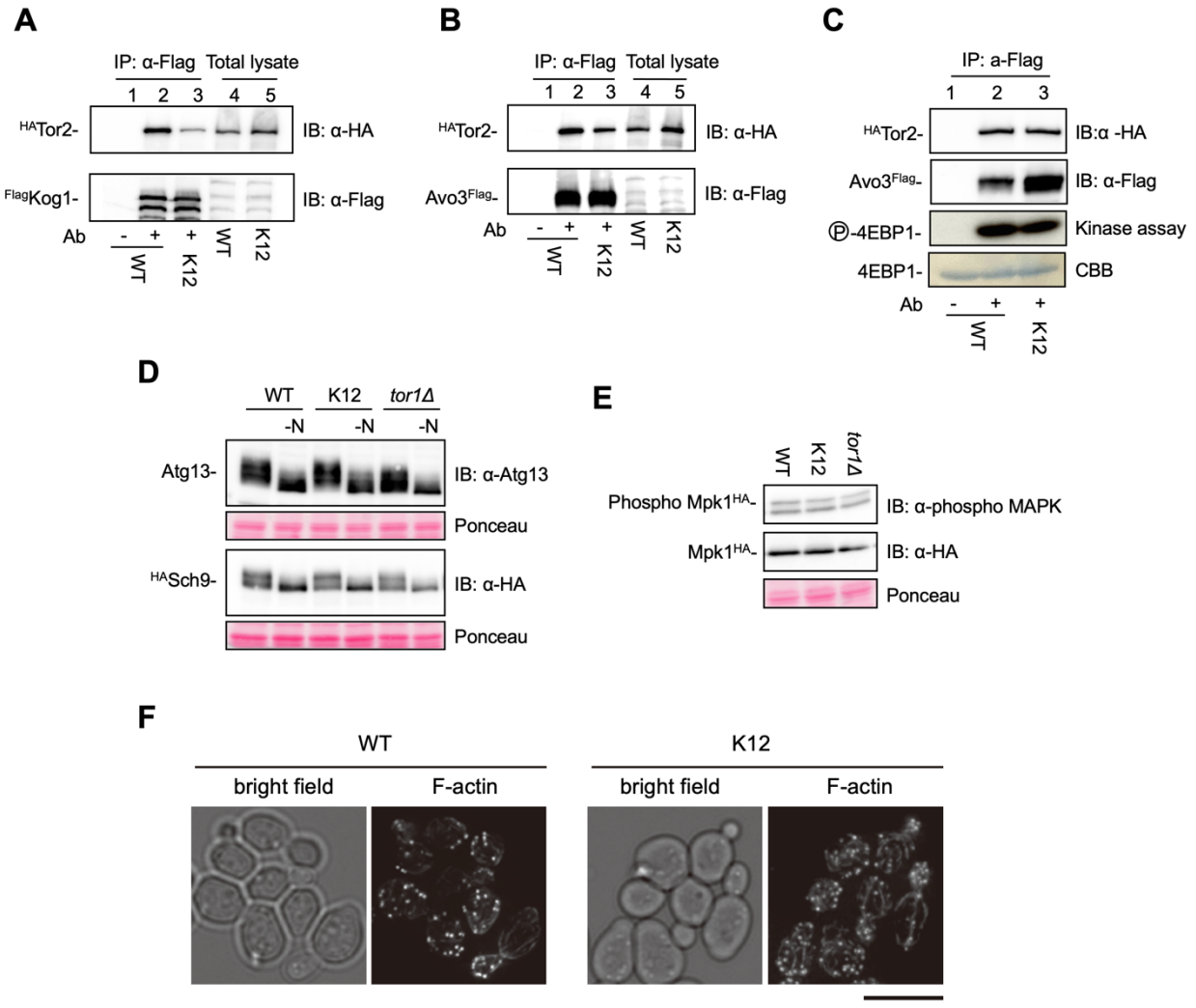

Fig. 4. Tor2(K12) mutant almost loses TORC1 assembling ability and retains TORC2 assembling ability.

A. Formation of Tor2-TORC1. ^{Flag}Kog1 was immunoprecipitated from cell lysate of the wildtype and *tor2*(K12) (lanes 4 and 5), and co-precipitated ^{HA}Tor2 in the immunocomplexes were detected (lane 1-3, lane 1 is immunoprecipitation control without antibody). *tor2*(K12) has almost no TORC1 assembling ability.

B. Formation of Tor2-TORC2. ^{Flag}Avo3 was immunoprecipitated from cell lysate (lanes 4 and 5), and co-precipitated ^{HA}Tor2 contained in the immunocomplexes was detected (lanes 1-3). *tor2*(K12) retains the TORC2 forming ability.

C. *In vitro* RI kinase assay of TORC2. The same amount of TORC2 was immunoprecipitated from cell lysate (estimated by the amount of ^{HA}Tor2 protein), and TORC2 kinase assay was carried out using 4EBP1 as a substrate. TORC2 kinase activity of Tor2(K12) is comparable with that of the wild-type Tor2. Non-RI kinase assay also yielded similar results (Appendix Fig. S2).

D. *In vivo* TORC1 kinase activities. Cells harbouring ATG13 (top) or ^{HA}SCH9 (bottom) plasmid growing in YEPD at 30 °C were treated by nitrogen starvation (-N) for 30 min, and the phosphorylation state of Atg13 and Sch9 was examined by immunoblotting. TORC1 in cells has similar activity to that of the wildtype.

E. *In vivo* TORC2 kinase activities. Cells harbouring MPK1^{HA} plasmid grown in YEPD at 30 °C were examined phosphorylation state of Mpk1 (top panel) by immunoblotting. TORC2 activity of Tor2(K12)-TORC2 in cells is also comparable to that of the wildtype.

F. Localization of F-actin in the *tor2*(K12) mutant. WT and *tor2*(K12) mutant cells were grown in YEPD at 30°C and processed for F-actin staining. Bright-field images are shown on the left. Scale bar, 5 μm.

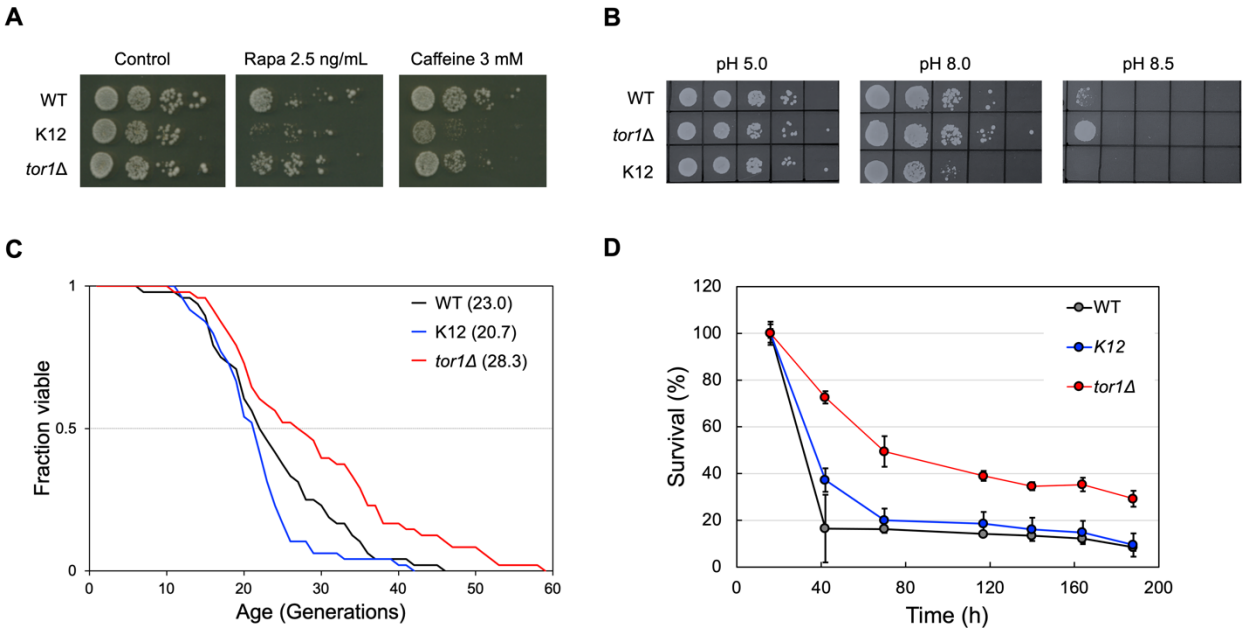

Fig. 5. Cell phenotypes induced by designing Tor2, K12.

A. Cell growth at various conditions, i.e., rapamycin and caffeine treatments. *tor2*(K12) strain has higher sensitivity for 2.5 ng/ml rapamycin (Rapa), a selective inhibitor of TORC1, and 3 mM caffeine, an inhibitor of TORC1.

B. Cell growth at indicated pH conditions (pH 5.0, 8.0, and 8.5). *tor1*Δ strain is viable at higher pH conditions and K12 strain is only viable at lower pH conditions, compared to the wildtype.

C. Replicative lifespans of the wild-type (Black), *tor2*(K12) (Blue), and *tor1*Δ (Red) strains. Mean life spans are shown in parentheses. Wilcoxon test, $p = 0.030$ (*tor1*Δ), $p = 0.20$ (K12); weighted log-rank test, $p = 0.0054$ (*tor1*Δ), $p = 0.065$ (K12) (versus wildtype).

D. Chronological lifespans of the wild-type (Black), *tor2*(K12) (Blue) and *tor1*Δ (Red) strains. Quantitative data in the figures represent the average ± standard deviation ($n = 3$). Deletion of Tor1-TORC1 extends the lifespans of both, while the deletion of Tor2-TORC1 has a small effect on their lifespans.

References

Allen JJ, Li M, Brinkworth CS, Paulson JL, Wang D, Hübner A, Chou W-H, Davis RJ, Burlingame AL, Messing RO *et al* (2007) A semisynthetic epitope for kinase substrates. *Nature methods* 4: 511-516

Baek M, DiMaio F, Anishchenko I, Dauparas J, Ovchinnikov S, Lee Gyu R, Wang J, Cong Q, Kinch Lisa N, Schaeffer RD *et al* (2021) Accurate prediction of protein structures and interactions using a three-track neural network. *Science* 373: 871-876

Chen K-YM, Keri D, Barth P (2020) Computational design of G Protein-Coupled Receptor allosteric signal transductions. *Nature Chemical Biology* 16: 77-86

Chino A, Watanabe K, Moriya H (2010) Plasmid Construction Using Recombination Activity in the Fission Yeast Schizosaccharomyces pombe. *PLOS ONE* 5: e9652

Dabrowska A, Kumar J, Rallis C (2022) Nutrient-Response Pathways in Healthspan and Lifespan Regulation. *Cells* doi: 10.3390/cells11091568 [PREPRINT]

Dauparas J, Anishchenko I, Bennett N, Bai H, Ragotte RJ, Milles LF, Wicky BIM, Courbet A, de Haas RJ, Bethel N *et al* (2022) Robust deep learning–based protein sequence design using ProteinMPNN. *Science* 378: 49-56

Dowling QM, Volkman HE, Gray EE, Ovchinnikov S, Cambier S, Bera AK, Sankaran B, Johnson MR, Bick MJ, Kang A *et al* (2023) Computational design of constitutively active cGAS. *Nature Structural & Molecular Biology*

Folch J, Busquets O, Ettcheto M, Sánchez-López E, Pallàs M, Beas-Zarate C, Marin M, Casadesus G, Olloquequi J, Auladell C *et al* (2018) Experimental Models for Aging and their Potential for Novel Drug Discovery. *Curr Neuropharmacol* 16: 1466-1483

Harrison DE, Strong R, Sharp ZD, Nelson JF, Astle CM, Flurkey K, Nadon NL, Wilkinson JE, Frenkel K, Carter CS *et al* (2009) Rapamycin fed late in life extends lifespan in genetically heterogeneous mice. *Nature* 460: 392-395

Hill A, Niles B, Cuyegkeng A, Powers T (2018) Redesigning TOR Kinase to Explore the Structural Basis for TORC1 and TORC2 Assembly. *Biomolecules* 8

Huang P-S, Boyken SE, Baker D (2016) The coming of age of de novo protein design. *Nature* 537: 320

Jumper J, Evans R, Pritzel A, Green T, Figurnov M, Ronneberger O, Tunyasuvunakool K, Bates

521 R, Žídek A, Potapenko A *et al* (2021) Highly accurate protein structure prediction with AlphaFold.
522 *Nature* 596: 583-589
523 Kaeberlein M, Powers RW, Steffen KK, Westman EA, Hu D, Dang N, Kerr EO, Kirkland KT,
524 Fields S, Kennedy BK (2005) Regulation of Yeast Replicative Life Span by TOR and Sch9 in
525 Response to Nutrients. *Science* 310: 1193
526 Kaiser C, Michaelis,S., & Mitchell, A. (1994) Methods in Yeast Genetics, A Cold Spring Harbor
527 Laboratory Course Manual. *Cold Spring Harbor Laboratory Press*
528 Kamada Y (2017) Novel tRNA function in amino acid sensing of yeast Tor complex1. *Genes to*
529 *Cells* 22: 135-147
530 Kamada Y, Fujioka Y, Suzuki Nobuo N, Inagaki F, Wullschleger S, Loewith R, Hall Michael N,
531 Ohsumi Y (2005) Tor2 Directly Phosphorylates the AGC Kinase Ypk2 To Regulate Actin
532 Polarization. *Molecular and Cellular Biology* 25: 7239-7248
533 Kamada Y, Funakoshi T, Shintani T, Nagano K, Ohsumi M, Ohsumi Y (2000) Tor-Mediated
534 Induction of Autophagy via an Apg1 Protein Kinase Complex. *Journal of Cell Biology* 150: 1507-
535 1513
536 Kamada Y, Yoshino K-i, Kondo C, Kawamata T, Oshiro N, Yonezawa K, Ohsumi Y (2010) Tor
537 Directly Controls the Atg1 Kinase Complex To Regulate Autophagy. *Molecular and Cellular*
538 *Biology* 30: 1049-1058
539 Kane PM (2006) The where, when, and how of organelle acidification by the yeast vacuolar H+-
540 ATPase. *Microbiol Mol Biol Rev* 70: 177-191
541 Kosugi T, Iida T, Tanabe M, Iino R, Koga N (2023) Design of allosteric sites into rotary motor
542 V1-ATPase by restoring lost function of pseudo-active sites. *Nature Chemistry* in press
543 Kunz J, Henriquez R, Schneider U, Deuter-Reinhard M, Movva NR, Hall MN (1993) Target of
544 rapamycin in yeast, TOR2, is an essential phosphatidylinositol kinase homolog required for G1
545 progression. *Cell* 73: 585-596
546 Leaver-Fay A, Tyka M, Lewis SM, Lange OF, Thompson J, Jacak R, Kaufman K, Renfrew PD,
547 Smith CA, Sheffler W *et al* (2011) ROSETTA3: an object-oriented software suite for the
548 simulation and design of macromolecules. *Methods in enzymology* 487: 545-574
549 Lin S-J, Defossez P-A, Guarente L (2000) Requirement of NAD and SIR2 for Life-Span Extension
550 by Calorie Restriction in Saccharomyces cerevisiae. *Science* 289: 2126-2128
551 Liu GY, Sabatini DM (2020) mTOR at the nexus of nutrition, growth, ageing and disease. *Nature*

Reviews Molecular Cell Biology 21: 183-203

Loewith R, Hall MN (2011) Target of Rapamycin (TOR) in Nutrient Signaling and Growth Control. *Genetics* 189: 1177-1201

Loewith R, Jacinto E, Wullschleger S, Lorberg A, Crespo JL, Bonenfant D, Oppliger W, Jenoe P, Hall MN (2002) Two TOR Complexes, Only One of which Is Rapamycin Sensitive, Have Distinct Roles in Cell Growth Control. *Molecular cell* 10: 457-468

Longtine MS, McKenzie A, 3rd, Demarini DJ, Shah NG, Wach A, Brachat A, Philippsen P, Pringle JR (1998) Additional modules for versatile and economical PCR-based gene deletion and modification in Saccharomyces cerevisiae. *Yeast* 14: 953-961

Ma H, Kunes S, Schatz PJ, Botstein D (1987) Plasmid construction by homologous recombination in yeast. *Gene* 58: 201-216

Martinez-Miguel VE, Lujan C, Espie--Caullet T, Martinez-Martinez D, Moore S, Backes C, Gonzalez S, Galimov ER, Brown AEX, Halic M *et al* (2021) Increased fidelity of protein synthesis extends lifespan. *Cell Metabolism* 33: 2288-2300.e2212

Nakajima T, Maruhashi T, Morimatsu T, Mukai Y (2020) Cyclin-dependent kinase Pho85p and its cyclins are involved in replicative lifespan through multiple pathways in yeast. *FEBS Letters* 594: 1166-1175

Nakano K, Toya M, Yoneda A, Asami Y, Yamashita A, Kamasawa N, Osumi M, Yamamoto M (2011) Pob1 Ensures Cylindrical Cell Shape by Coupling Two Distinct Rho Signaling Events During Secretory Vesicle Targeting. *Traffic* 12: 726-739

Nelson H, Nelson N (1990) Disruption of genes encoding subunits of yeast vacuolar H(+)-ATPase causes conditional lethality. *Proceedings of the National Academy of Sciences* 87: 3503-3507

Ohtsuka H, Kobayashi M, Shimasaki T, Sato T, Akanuma G, Kitaura Y, Otsubo Y, Yamashita A, Aiba H (2021a) Magnesium depletion extends fission yeast lifespan via general amino acid control activation. *MicrobiologyOpen* 10: e1176

Ohtsuka H, Shimasaki T, Aiba H (2021b) Extension of chronological lifespan in Schizosaccharomyces pombe. *Genes to Cells* 26: 459-473

Otsubo Y, Nakashima A, Yamamoto M, Yamashita A (2017) TORC1-Dependent Phosphorylation Targets in Fission Yeast. *Biomolecules* doi: 10.3390/biom7030050 [PREPRINT]

Prouteau M, Bourgoint C, Felix J, Bonadei L, Sadian Y, Gabus C, Savvides SN, Gutsche I, Desfosses A, Loewith R (2023) EGOC inhibits TOROID polymerization by structurally activating

583 TORC1. *Nature Structural & Molecular Biology*
584 Ratto E, Chowdhury SR, Siefert NS, Schneider M, Wittmann M, Helm D, Palm W (2022) Direct
585 control of lysosomal catabolic activity by mTORC1 through regulation of V-ATPase assembly.
586 *Nature Communications* 13: 4848
587 Reinke A, Anderson S, McCaffery JM, Yates J, Aronova S, Chu S, Fairclough S, Iverson C,
588 Wedaman KP, Powers T (2004) TOR Complex 1 Includes a Novel Component, Tco89p
589 (YPL180w), and Cooperates with Ssd1p to Maintain Cellular Integrity in Saccharomyces
590 cerevisiae*. *Journal of Biological Chemistry* 279: 14752-14762
591 Reinke A, Chen JCY, Aronova S, Powers T (2006) Caffeine Targets TOR Complex I and Provides
592 Evidence for a Regulatory Link between the FRB and Kinase Domains of Tor1p*. *Journal of*
593 *Biological Chemistry* 281: 31616-31626
594 Rodríguez-López M, Gonzalez S, Hillson O, Tunnacliffe E, Codlin S, Tallada VA, Bähler J, Rallis
595 C (2020) The GATA Transcription Factor Gaf1 Represses tRNAs, Inhibits Growth, and Extends
596 Chronological Lifespan Downstream of Fission Yeast TORC1. *Cell Reports* 30: 3240-3249.e3244
597 Scaiola A, Mangia F, Imseng S, Boehringer D, Berneiser K, Shimobayashi M, Stuttfeld E, Hall
598 MN, Ban N, Maier T (2020) The 3.2-Å resolution structure of human mTORC2. *Science Advances*
599 6: eabc1251
600 Sekiguchi T, Kamada Y, Furuno N, Funakoshi M, Kobayashi H (2014) Amino acid residues
601 required for Gtr1p-Gtr2p complex formation and its interactions with the Ego1p-Ego3p complex
602 and TORC1 components in yeast. *Genes to Cells* 19: 449-463
603 Sung H, Chul Han K, Chul Kim J, Oh KW, Su Yoo H, Tae Hong J, Bok Chung Y, Lee C-k, Lee
604 KS, Song S (2005) A set of epitope-tagging integration vectors for functional analysis in
605 Saccharomyces cerevisiae. *FEMS Yeast Research* 5: 943-950
606 Takahara T, Hara K, Yonezawa K, Sorimachi H, Maeda T (2006) Nutrient-dependent
607 Multimerization of the Mammalian Target of Rapamycin through the N-terminal HEAT Repeat
608 Region*. *Journal of Biological Chemistry* 281: 28605-28614
609 Tsverov J, Yegorov K, Powers T (2022) Identification of defined structural elements within TOR2
610 kinase required for TOR complex 2 assembly and function in Saccharomyces cerevisiae. *Mol Biol*
611 *Cell* 33: ar44
612 Urban J, Soulard A, Huber A, Lippman S, Mukhopadhyay D, Deloche O, Wanke V, Anrather D,
613 Ammerer G, Riezman H *et al* (2007) Sch9 Is a Major Target of TORC1 in *Saccharomyces*

cerevisiae. *Molecular cell* 26: 663-674

Waterhouse A, Bertoni M, Bienert S, Studer G, Tauriello G, Gumienny R, Heer FT, de Beer TA P, Rempfer C, Bordoli L *et al* (2018) SWISS-MODEL: homology modelling of protein structures and complexes. *Nucleic Acids Research* 46: W296-W303

Yang H, Jiang X, Li B, Yang HJ, Miller M, Yang A, Dhar A, Pavletich NP (2017) Mechanisms of mTORC1 activation by RHEB and inhibition by PRAS40. *Nature* 552: 368-373